

# Well-Defined Phase Sequence Including Cholesteric, Smectic A, and Columnar Phases Observed in a Thermotropic LC System of Simple Rigid-Rod Helical Polysilane

Kento Okoshi,<sup>\*,†,§</sup> Hiroyuki Kamee,<sup>†</sup> Goro Suzuki,<sup>†</sup> Masatoshi Tokita,<sup>†</sup> Michiya Fujiki,<sup>‡,§</sup> and Junji Watanabe<sup>†,§</sup>

Department of Polymer Chemistry, Tokyo Institute of Technology, Ookayama, Meguro-ku, Tokyo 152-8552, Japan; Graduate School of Materials Science, Nara Institute of Science and Technology, 8916-5 Takayama, Ikoma, Nara 630-0101, Japan; and CREST-JST (Japan Science and Technology Corporation), 4-1-8 Hon-cho, Kawaguchi, Saitama 332-0012, Japan

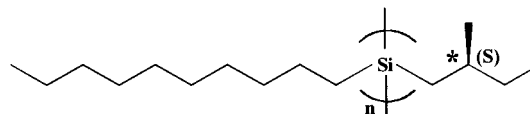
Received November 26, 2001

Revised Manuscript Received March 7, 2002

Liquid crystal phases formed by rigid-rod polymers have been studied extensively in both theoretical and experimental ways. In the initial stage of theoretical approach, it has been shown that a system of long, hard molecules can exhibit an orientationally ordered nematic phase if the density is efficiently high.<sup>1</sup> Recently, computer simulation has played an important role in understanding the liquid crystalline behavior of systems composed of hard rod molecules and has given the first indication that the smectic and columnar phases can also be formed by systems of molecules that interact through excluded-volume interaction alone.<sup>2</sup> Prior to this simulation, it was thought that smectic phases could only be exhibited by conventional molecules composed of aromatic mesogen groups and aliphatic tail groups which exhibit mainly attractive interactions.<sup>3</sup> This prompted many further theoretical studies of simple hard-rod systems.<sup>4–6</sup> On the experimental side, lyotropic phases have been extensively studied in biological molecular systems. The columnar and smectic liquid crystals have been reported in lyotropic liquid crystals of synthetic polypeptides,<sup>7</sup> DNA,<sup>8</sup> and the tobacco mosaic virus.<sup>9</sup> These liquid crystal phases observed can be easily differentiated from nematic and cholesteric phases which have so far been well studied for these kinds of rodlike polymers, but the detailed identification and nature of these new phases are still unclear because of the difficulty in managing the lyotropic system.

In this study, we treat the polysilanes with chiral side chains that assume a helical rigid-rod conformation with the persistent length of around 85 nm. The rigidity results from severe restriction of main chain's internal rotation by steric hindrance between neighboring side chains.<sup>10,11</sup> Such polymer chain stiffness is closely correlated to the liquid crystallinity in the lyotropic system. Here, we find that these helical polysilanes can form thermotropic liquid crystals (LCs) as well as the lyotropic LCs if the long alkyl side chains are attached to the main chain as a second side group, as reported in a previous study.<sup>12</sup> The ability of thermotropic LC formation is due to the long flexible side chains that act

as solvents in the lyotropic system.<sup>13</sup> A typical polysilane that forms a thermotropic liquid crystal is poly[*n*-decyl-(*S*)-2-methylbutylsilane] (PD2MBS) with the following formula:



This PD2MBS polymer, having length  $1.96 \times n \text{ \AA}$  ( $n$ : degree of polymerization) and diameter 15 Å, can be an ideal molecule to use to verify the theoretical predictions of the hard-rod model because the molecules interact mainly through excluded-volume interactions because no significant electrostatic intermolecular attractions are present due to its nonpolar nature. The nonpolar nature is also advantageous for the preparation of a sample with a narrow molecular weight distribution. A simple fractional precipitation method can be used due to the lack of aggregation by the molecules in solution. The results show that the thermotropic phase behavior strongly depends on the polydispersity of molecular length. Materials with a wider distribution of molecular weight form a cholesteric liquid crystal.<sup>14</sup> On the other hand, carefully fractionated materials with a narrow distribution of molecular weight form a smectic A (SmA) liquid crystal. Some materials with an intermediate distribution show the cholesteric–SmA transition with decreasing temperature. In the temperature region below that of these fluid phases, the columnar liquid crystal exists in a form of a milky wax. This phase sequence, which includes cholesteric, SmA, and columnar phases, is similar to that predicted theoretically by considering the excluded-volume effect of hard-rod molecules. The study of the step-by-step organization of rodlike polymers is of considerable interest for the purpose of understanding the self-organization of molecules in biological systems<sup>15</sup> and manipulating the processing of nanoscaled materials.

PD2MBS was synthesized with dichlorosilane monomer bearing (*S*)-2-methylbutyl and *n*-decyl substituents by the Wurtz-type condensation in toluene at 120 °C.<sup>10</sup> In this hard-rod system, the axial ratio and polydispersity of length, which has never been seriously considered in previous studies,<sup>10,11,13</sup> are crucial to realize the nature of predicted and observed liquid crystal phases. Thus, the synthesized samples in toluene solution were repeatedly fractionated by the fractional precipitation method with 2-propanol, ethanol, and methanol as precipitants. The molecular weights of the resulting polymers were determined by gel permeation chromatography (GPC) with a column of Shodex K-2004, using chloroform at 40 °C as an eluent and with calibration by polystyrene standards. Almost 20 samples prepared have molecular weights ranging from 10 000 to 50 000 and the polydispersity,  $M_w/M_n$ , ranging from 1.05 to 1.25.

All of the samples are similar in appearance and texture to milky wax when at room temperature. The X-ray diffraction pattern from this room temperature phase revealed several reflections (see Figure 2a), which have spacings of 17.9, 14.6, 12.0, 10.0, and 8.5 Å. All these reflections were assigned to orthogonal molecular

<sup>†</sup> Tokyo Institute of Technology.

<sup>‡</sup> Nara Institute of Science and Technology.

<sup>§</sup> CREST-JST.

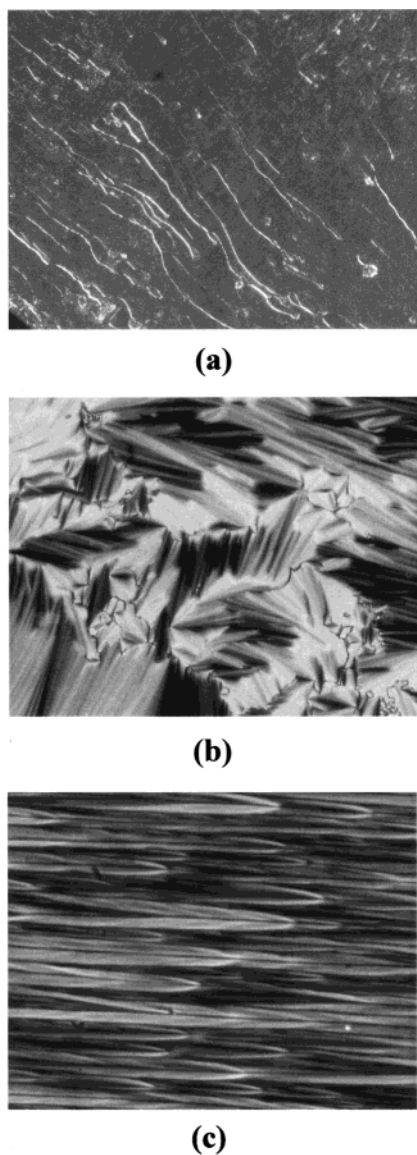


**Figure 1.** Polarizing optical micrographs. (a) Typical Grandjean texture including partly oily streaks that is taken at 100 °C of PD2MBS with  $M_w = 10\,400$  and  $M_w/M_n = 1.16$  in the parallel glass cell. (b) Fan shape texture taken at 100 °C for PD2MBS with  $M_w = 19\,300$  and  $M_w/M_n = 1.11$ . (c) Oriented fan texture observed for the same sample as in (b). The orientation was performed by shearing along the vertical direction. The observations were performed with an Olympus BH-2 polarizing microscopy equipped with a Mettler FP82 hot stage.

packing with a two-dimensional lattice of  $a = 17.9$  Å,  $b = 24.0$  Å, and  $\gamma = 90^\circ$ . In the oriented pattern, only the quasi-meridional streak and the meridional reflections with spacings of 4.4 and 1.96 Å, respectively, can be recorded. These are attributed to the 7-residue 3-turn ( $7_3$ ) helical conformation with a repeat length of 1.96 Å; the 4.4 Å streak is assigned to a 3rd turn-layer line, and the 1.96 Å reflection is a meridional one just on a 7th layer line.<sup>16</sup> The lack of the layer reflections shows the random displacement of molecules along the chain axis. Density requires that two chains run through the unit cell. It is therefore concluded that the room temperature phase is a columnar liquid crystal phase.

On heating, the waxlike material begins to flow spontaneously at a certain temperature, which is determined by the molecular weight of the PD2MBS. Simultaneously, the sharp equatorial reflections become

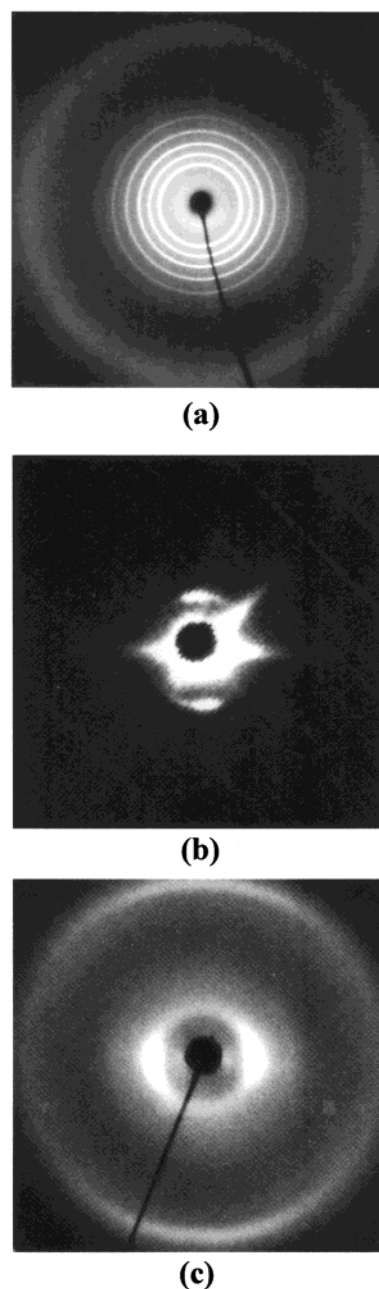


**Figure 2.** (a) Wide-angle X-ray pattern taken at room temperature of the low-temperature columnar phase of the material with  $M_w = 9900$  and  $M_w/M_n = 1.15$ . (b) Small-angle X-ray pattern and (c) wide-angle X-ray pattern taken at 100 °C of the oriented smectic phase of the material with  $M_w = 37\,500$  and  $M_w/M_n = 1.10$ . The orientation was achieved by shearing the SmA in the horizontal direction. The samples for these measurements were kept between thin glasses and heated to the desired temperature with a Mettler FP82 hot stage. The X-ray patterns were recorded with a flat-plate camera using a Rigaku-Denki X-ray generator with Ni-filtered Cu K $\alpha$  radiation.

diffuse. Only the broad reflection with the 15 Å spacing is distinguishable on the equatorial line whereas the outer 4.4 and 1.96 Å reflections characteristic of the  $7_3$  helical conformation still remain. These can be expected for a conventional liquid crystal, in which the molecules are laterally packed with a liquid nature. A DSC thermogram also shows a very small peak on the same transition. The transition temperatures, as determined from the DSC and X-ray, are increased with the increased molecular weight from 60 °C for the material

with the lowest  $M_n = 10\,000$  and  $180\text{ }^\circ\text{C}$  for the material with the highest  $M_n = 50\,000$ .

The fluid phases exhibit the strong birefringence and characteristic texture precisely indicative of the conventional fluid liquid crystals. Figure 1a shows a polarizing optical micrograph of the sample with  $M_w = 10\,400$  and  $M_w/M_n = 1.16$  taken at  $100\text{ }^\circ\text{C}$ . It shows the Grandjean planar texture including partly oily streaks. Simultaneously, it shows the reflection colors changing from blue to red on heating.<sup>14</sup> The reciprocal pitch changes proportionally to the absolute temperature. This is just indicative of the cholesteric helical phase. The cholesteric nature is sustained at the higher temperature until the decomposition temperature at around  $250\text{ }^\circ\text{C}$ .

It is interesting that the fluid cholesteric liquid crystal disappears and that the smectic phase appears when the molecular weight distribution of materials becomes narrow. Figure 1b shows the microphotograph of the smectic phase observed for the material with  $M_w = 19\,300$  and  $M_w/M_n = 1.11$ . The well-known fan-shaped texture characteristic of the smectic layer structure can be seen. The behavior of the orientation by shearing is also completely different from that in the cholesteric liquid crystal. By shearing, the extinction of light was observed between the crossed polarizers when one of the polarizers was parallel to the shearing direction, but the smectic focal-conic textures are oriented with the disclination lines perpendicular to the shearing direction (see Figure 1c). This can be understood if the smectic layers are oriented parallel and so the molecules are aligned perpendicular to the shearing direction. The decisive evidence of the smectic layer structure is given from the small-angle X-ray diffraction pattern. Figure 2b shows the photograph taken of the oriented smectic phase of the material with  $M_w = 37\,500$  and  $M_w/M_n = 1.10$ . It shows a sharp reflection with the spacing of  $266\text{ }\text{\AA}$  in a meridional direction, which is perpendicular to the shearing direction. The spacing is not dependent on the temperature and corresponds to the molecular length that is calculated with  $M_n$  and the translational unit length per residue,  $1.96\text{ }\text{\AA}$ . For the same oriented sample, the outer broad reflections with the spacing of  $15\text{ }\text{\AA}$  attributable to the lateral packing of molecules lie in an equatorial direction as observed in Figure 2c. These indicate the SmA modification, where the hard-rod molecules form the layer with their ends, which are placed at a confined space, and their long axes perpendicular to the layer. The smectic layer spacings collected from the several fractionated samples are plotted against the length of molecules calculated from the  $M_n$  in Figure 3. A good correspondence between the observed and calculated lengths can be found.

One can easily envisage that the SmA ordering is disfavored when the polydispersity is large, since the rods of different lengths do not pack into layers as effectively as rods of the same length. In fact, a theoretical study that treats polydispersity in hard-rod length predicted that the nematic phase stabilizes with increasing polydispersity and the smectic phase is depleted at a certain polydispersity.<sup>17</sup> This expected effect can be clearly found from Figure 4 where the materials forming SmA and cholesteric phases are presented as closed and open circles, respectively, on the map with the  $M_w$  and  $M_w/M_n$  coordinates. It is obvious that the SmA materials are placed in a certain part where the molecular weight distribution is relatively sharp. The critical polydispersity above which the SmA phase is no

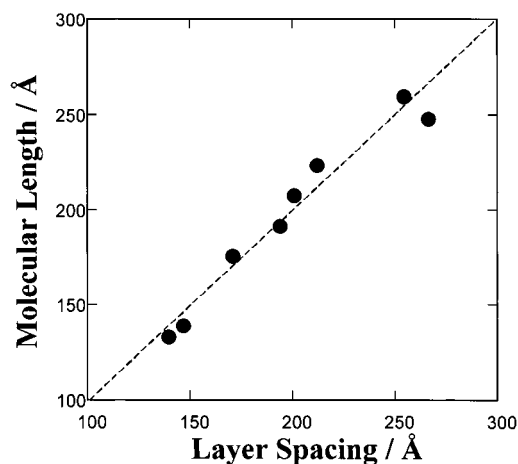


**Figure 3.** Comparison of the layer spacing elucidated from the small-angle X-ray method and the molecular length calculated with  $M_n$  and  $1.96\text{ }\text{\AA}$  as a translational repeat length per residue.

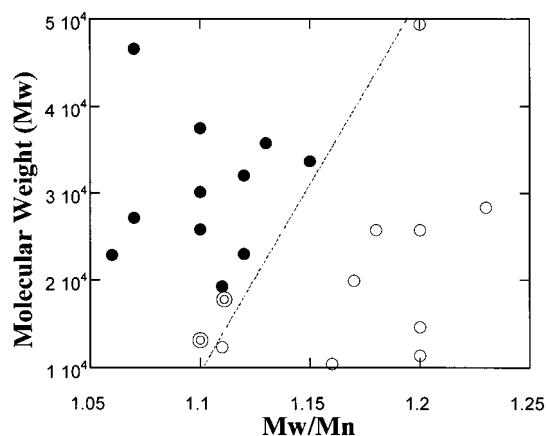


**Figure 4.** Schematic plots of materials on the map with the coordinates of the molecular weight,  $M_w$ , and the polydispersity,  $M_w/M_n$ . Open and closed circles stand for the materials forming cholesteric and SmA phases, respectively. The materials given by double circles form the cholesteric and SmA phases in order of decreasing temperature.

longer stable is around 1.15, although it becomes somewhat larger when the average molecular weight increases (refer to the dotted line in Figure 4). Finally, it should be noted that some samples denoted by double circles, which have the polydispersity slightly sharper than the critical value, show the cholesteric–smectic A–columnar phase transformations in order of decreasing temperature. The polymorphism in this phase sequence coincides with the theoretical prediction.<sup>2,4–6,17</sup>

These results show the well-defined thermotropic phase behavior in a simple hard-rod polysilane, in which the excluded-volume interaction significantly works. Especially, the first clear identification of the SmA phase in the thermotropic system is interesting, since the molecules can be arranged with their ends located at a confined space in a fluid thermotropic LC field. Combining with some attractive interaction, which can be produced by attaching the polar side chains, will provide the possibility of many types of smectic liquid crystals, i.e., many kinds of self-assemble structures, even in the simple hard-rod polymers, which are completely different from the conventional thermotropic molecules. This study suggests a new field of the thermotropic LC composed of the hard-rod molecules.

## References and Notes

- (1) Onsager, L. *Ann. N.Y. Acad. Sci.* **1949**, *51*, 627–659. Flory, P. J. *Proc. R. Soc. London* **1956**, *A234*, 60–89.
- (2) Frenkel, D.; Lekkerkerker, H. N. W.; Stroobants, A. *Nature (London)* **1988**, *332*, 822–823.
- (3) Gray, G. W. In *Smectic Liquid Crystals*; Leonard Hill: 1984.
- (4) Kimura, H.; Tsuchiya, M. *J. Phys. Soc. Jpn.* **1990**, *59*, 3563–3570.
- (5) Hentschke, R.; Hertfeld, J. *Phys. Rev.* **1991**, *A44*, 1148–1155.
- (6) Bolhuis, P. G.; Frenkel, D. *J. Chem. Phys.* **1997**, *106*, 666–687.
- (7) Lee, S.; Meyer, R. B. *Liq. Cryst.* **1990**, *7*, 451–455. Livolant, F.; Bouligand, Y. *J. Phys. (Paris)* **1986**, *47*, 1813–1827. Watanabe, J. In *Ordering in Macromolecular Systems*; Teramoto, A., Kobayashi, M., Norisue, T., Eds.; Springer: Berlin, 1993; p 99. Watanabe, J.; Takashina, Y. *Macromolecules* **1991**, *24*, 3423–3426. Tirrell, D. A.; et al. *Nature (London)* **1997**, *389*, 167–170.
- (8) Strzelecka, T. E.; Davidson, M. W.; Rill, R. L. *Nature (London)* **1988**, *331*, 457–460. Livolant, F.; Levelut, A. M.; Doucet, J.; Benoit, J. P. *Nature (London)* **1989**, *339*, 724–726.
- (9) Wen, X.; Meyer, R. B.; Caspar, D. L. D. *Phys. Rev. Lett.* **1989**, *63*, 2760–2763.
- (10) Fujiki, M. *J. Am. Chem. Soc.* **1996**, *118*, 7424–7425.
- (11) Terao, K.; Terao, Y.; Teramoto, A.; Nakamura, N.; Terakawa, I.; Sato, T.; Fujiki, M. *Macromolecules* **2001**, *34*, 2682–2685.
- (12) Asuke, T.; West, R. *Macromolecules* **1991**, *24*, 343–344.
- (13) Watanabe, J.; Ono, J.; Uematsu, I.; Abe, A. *Macromolecules* **1985**, *18*, 2141–2148.
- (14) Watanabe, J.; Kamee, H.; Fujiki, M. *Polym. J.* **2001**, *33*, 495–497.
- (15) Neville, A. C. In *Biology of Fibrous Composites*; Cambridge University Press: New York, 1993.
- (16) Miller, R. D.; Farmer, B. L.; Fleming, W.; Sooriyakumaran, R.; Rabolt, J. *J. Am. Chem. Soc.* **1987**, *109*, 2509–2510.
- (17) Bates, M. A.; Frenkel, D. *J. Chem. Phys.* **1998**, *109*, 6193–6199.

MA012056Z